Current Biology 20, 521–526, March 23, 2010 ©2010 Elsevier Ltd All rights reserved DOI 10.1016/j.cub.2010.01.046

Report

p53 Prevents Entry into Mitosis with Uncapped Telomeres

Maria Thanasoula,[1] Jose Miguel Escandell,[1] Paula Martinez,[2] Sophie Badie,[1] Purificacion Muñoz,[2,3] María A. Blasco,[2] and Madalena Tarsounas[1,*]

[1]Telomere and Genome Stability Group, The CR-UK/MRC Gray Institute for Radiation Oncology and Biology, Old Road Campus, Oxford OX3 7DQ, UK

[2]Telomeres and Telomerase Group, Molecular Oncology Program, Spanish National Cancer Center (CNIO), Madrid E-28029, Spain

Summary

Telomeres are protected by capping structures consisting of core protein complexes that bind with sequence specificity to telomeric DNA (reviewed in [1]). In their absence, telomeres trigger a DNA damage response, materialized in accumulation at the telomere of damage response proteins, e.g., phosphorylated histone H2AX (γH2AX), into telomere-dysfunction-induced foci [2, 3]. Telomere uncapping occurs transiently in every cell cycle in G2 [4], following DNA replication, but little is known about how protective structures are reassembled or whether this process is controlled by the cell-cycle surveillance machinery. Here, we report that telomere capping is monitored at the G2/M transition by the p53/p21 damage response pathway. Unlike their wild-type counterparts, human and mouse cells lacking p53 or p21 progress into mitosis prematurely with persisting uncapped telomeres. Furthermore, artificially uncapped telomeres delay mitotic entry in a p53- and p21-dependent manner. Uncapped telomeres that persist in mitotic p53-deficient cells are shorter than average and religate to generate end-to-end fusions. These results suggest that a p53-dependent pathway monitors telomere capping after DNA replication and delays G2/M progression in the presence of unprotected telomeres. This mechanism maintains a cell-cycle stage conducive for capping reactions and prevents progression into stages during which uncapped telomeres are prone to deleterious end fusions.

Results and Discussion

DNA Damage Response Factors at Human Telomeres during Mitosis

Telomere uncapping leads to checkpoint activation and recruitment of DNA damage response factors to the telomere (e.g., 53BP1, MDC1, γH2AX, and ATM), visualized as microscopically defined telomere-dysfunction-induced foci (TIFs, reviewed in [5]). Telomeres become transiently uncapped in every cell cycle following their replication in S phase, and the ensuing ATM-dependent response is thought to promote the reassembly of protective telomeric structures in G2 [4]. To monitor telomere recapping at the G2/M transition under physiological conditions, we synchronized human HeLa 1.2.11 cells by double thymidine block and release. γH2AX foci were detectable in G2, and a subset of these localized to telomeres, indicative of TIFs (see Figure S1A, available online). Upon entry into mitosis, several sites of γH2AX labeling persisted, and these preferentially colocalized with telomeres labeled with an anti-TRF2 antibody (Figure 1A). The frequency of these mitotic TIFs was comparable to that of interphase TIFs (Figures S1A), suggestive of persistence of G2-uncapped telomeres into mitosis. To confirm γH2AX localization at telomeres, we visualized TIFs on mitotic chromosomes by colocalization of γH2AX and telomeric fluorescent in situ hybridization (FISH) signals (Figures 1B and 1C). In addition to γH2AX, we also detected MDC1 at mitotic telomeres (Figure S1B), a damage response mediator at the G2/M transition [6]. In contrast, 53BP1, another damage response protein [7], was not detected at mitotic telomeres. HeLa 1.2.11 cells carry relatively long telomeres (~17 kb [8]). We therefore also analyzed HeLa OHIO cells with shorter telomeres (~3.4 kb [8]) and again observed γH2AX labeling of mitotic telomeres (Figures 1B and 1C). The number of γH2AX-labeled telomeres in mitotic HeLa OHIO cells was even higher than in HeLa 1.2.11 cells (Figure 1D).

γH2AX staining at deprotected telomeres can extend over approximately 570 kb into the subtelomeric region in human cells [9]. Consistently, the chromatin domain covered by γH2AX often extended beyond the telomeric FISH signal or the region of TRF2 staining in our experiments (Figures 1A–1C). To address whether the γH2AX signal indeed originated from telomeric DNA, we analyzed γH2AX binding to telomere DNA by using chromatin immunoprecipitation (ChIP; Figure 2A). We used HeLa 1.2.11 cells either untreated or arrested in mitosis by addition of colcemid. An antibody against γH2AX efficiently pulled down telomeric DNA from mitotic cells, whereas less enrichment was observed in unsynchronized cells. An antibody against the telomere-associated protein TRF2 was used as a positive control that precipitated telomeric DNA with similar yield in both cases. Preimmune serum served as a control for nonspecific binding, and no precipitation was observed when a nontelomeric rDNA probe was used instead of a telomere probe for detection. These results confirm specific association of γH2AX with telomeres, which can clearly be seen in cells arrested in mitosis.

Mitotic TIFs Mark Short, Uncapped Telomeres

We next addressed whether a correlation existed between telomere length and the occurrence of mitotic TIFs. Our initial results suggested that HeLa OHIO cells with shorter telomeres show a somewhat higher incidence of telomeric γH2AX staining during mitosis compared to HeLa 1.2.11 cells (Figure 1D). This observation was confirmed in mitotic chromosome preparations of HeLa 1.2.11 cells, where we observed that nuclei with stronger telomeric FISH signals, indicative of long telomeres (Figure 2B, long), typically lack TIFs. In contrast, TIFs were abundant in metaphases with shorter telomeres, on the basis of the FISH signal intensity (Figure 2B, short). To quantitatively assess whether γH2AX labeling was linked to short telomere length, we measured the intensities of individual

*Correspondence: madalena.tarsounas@rob.ox.ac.uk

[3]Present address: Epigenetics and Cancer Biology Program (PEBC), Catalan Institute of Oncology (ICO), Gran Via s/n, 08907 L'Hospitalet de Llobregat, Barcelona, Spain

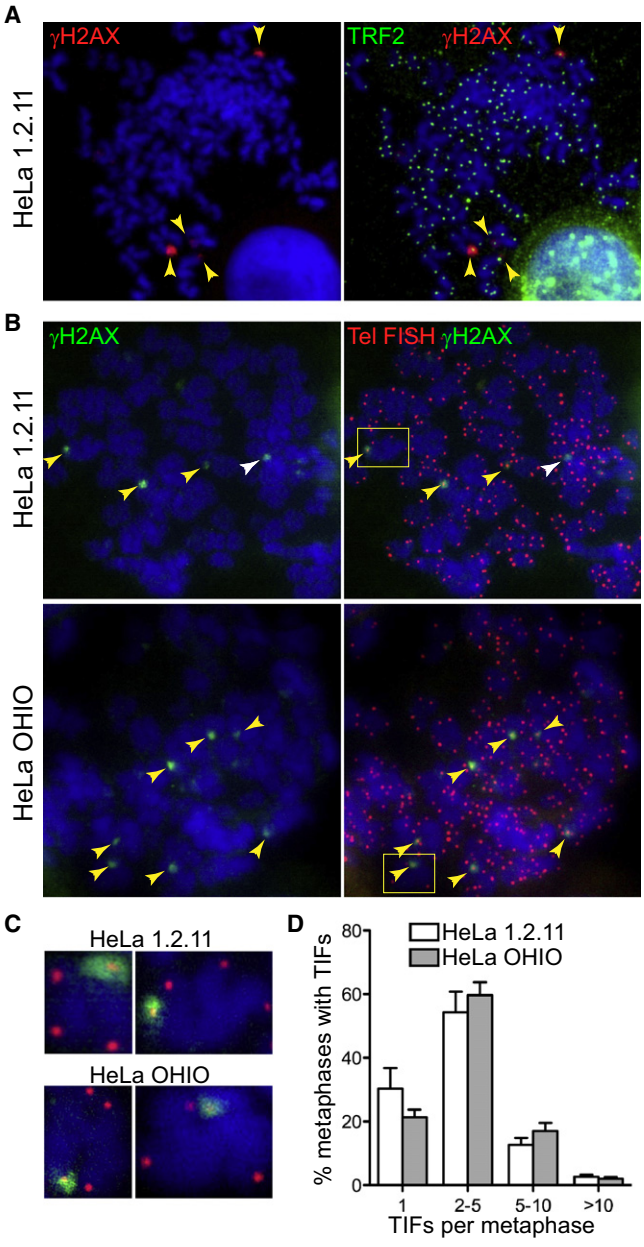

Figure 1. γH2AX Persists at Telomeres during Mitosis

(A) HeLa 1.2.11 cells were arrested in mitosis with colcemid treatment and mitotic chromosomes spread onto glass slides. Preparations were stained with anti-TRF2 (green) and anti-γH2AX antibodies (red). DNA was counterstained with DAPI (blue).

(B) Mitotic chromosomes isolated from HeLa 1.2.11 and HeLa OHIO cells arrested in mitosis with colcemid were spread onto glass slides via the cytospin method. Preparations were fixed and stained with anti-γH2AX monoclonal antibody (green). Telomeres were visualized with a Cy3-conjugated $(CCCTAA)_6$-PNA probe (red). Yellow arrows indicate TIFs. White arrows point at γH2AX foci that do not colocalize with telomeres.

(C) Enlarged images, including the areas marked with yellow rectangles in (B).

(D) Quantification of TIFs in HeLa 1.2.11 and HeLa OHIO cells. One hundred metaphases were scored for each cell line. Error bars represent standard deviation (SD) of three independent experiments.

This figure is related to Figures S1 and S2.

telomeric FISH signals in mitotic HeLa 1.2.11 cells by using the Q-FISH technique and recorded their γH2AX status in the same preparation. This revealed that shorter telomeres were indeed more likely to be labeled by γH2AX. Twenty percent of γH2AX-positive telomeres, but only 7% of all telomeres, were shorter than 10 kb in length (Figure 2B).

To determine whether mitotic γH2AX labeling is indicative of uncapped telomeres, we artificially created telomere uncapping by overexpression of dominant-negative TRF2 lacking both Myb and N-terminal basic domain ($TRF2^{\Delta M\Delta B}$ [10]) in human T4 cells under control of a doxycyclin-repressible promoter. $TRF2^{\Delta M\Delta B}$ levels increased over 7 days after removal of doxycyclin from the growth medium (Figure 2C). Before induction, only a few TIFs were detected on spread metaphase chromosomes, similar to what we observed in HeLa cells. In contrast, 7 days after induction of $TRF2^{\Delta M\Delta B}$, the majority of mitotic telomeres were labeled by γH2AX (Figure 2C). We conclude that uncapped telomeres display mitotic γH2AX staining. TIFs persisting into mitosis in cells with intact telomere structure may therefore reflect telomeres that have remained uncapped after their replication in S phase.

The p53/p21 Pathway Prevents Mitotic Entry with Uncapped Telomeres and Telomere Fusion

Telomere capping after DNA replication is thought to be completed during the G2 phase of the cell cycle [4]; therefore, the widespread presence of mitotic TIFs in a range of human cell lines came as a surprise. However, the cells so far used in our studies lacked functional p53. To investigate whether p53 plays a role in preventing mitotic uncapped telomeres, we first analyzed the human U2OS cell line that is proficient for p53 function [11]. γH2AX labeling on mitotic chromosomes was rarely seen but increased to frequencies similar to HeLa cells after siRNA-mediated depletion of p53 or p21 from these cells (Figure S2). To confirm the dependence of mitotic TIFs on the *p53* status, we analyzed isogenic mouse embryonic fibroblasts (MEFs) carrying wild-type *p53* or a targeted deletion in the *p53* gene [12]. γH2AX labeling of mitotic chromosomes was again rarely seen in wild-type MEFs but occurred frequently in $p53^{-/-}$ MEFs (Figure 3A). As was the case in human HeLa cells, Q-FISH analysis revealed that γH2AX staining was preferentially observed at short telomeres of $p53^{-/-}$ MEFs (data not shown). These results suggest that p53 is required either for efficient capping of telomeres in G2 before the time of mitotic entry or to prevent progression into mitosis while telomere capping reactions are ongoing. p53 has been shown to delay mitotic entry in response to DNA damage by upregulation of its downstream target p21 [13]. We observed mitotic TIFs in MEFs carrying a *p21* deletion [14] as frequently as in MEFs lacking *p53* (Figure 3A). This suggests that one role of p53 is to delay cell-cycle progression into mitosis by p21 induction when uncapped telomeres persist. Association of γH2AX with sites close to the telomeres of mitotic chromosomes has been reported in late generation $Terc^{-/-}$ T cells [15]. When we quantified mitotic TIFs in $Terc^{-/-}$ shp53 MEFs [16] with short telomeres (G4; ~20.88 kb average), we found a substantial increase compared to wild-type MEFs (~36.4 kb average) (Figures 3A and 3B). This confirms our observation that shorter telomeres are more prone to persisting in an uncapped state.

To obtain insight into the fate of uncapped telomeres in the absence of p53, we examined the frequency of chromosome abnormalities in $p53^{-/-}$ MEFs (Figure 3C). As expected, we observed an increased incidence of DNA breaks and complex structural aberrations in $p53^{-/-}$ MEFs, as compared to $p53^{+/+}$ MEFs established from three embryos derived for each genotype (data not shown). In addition, we observed an

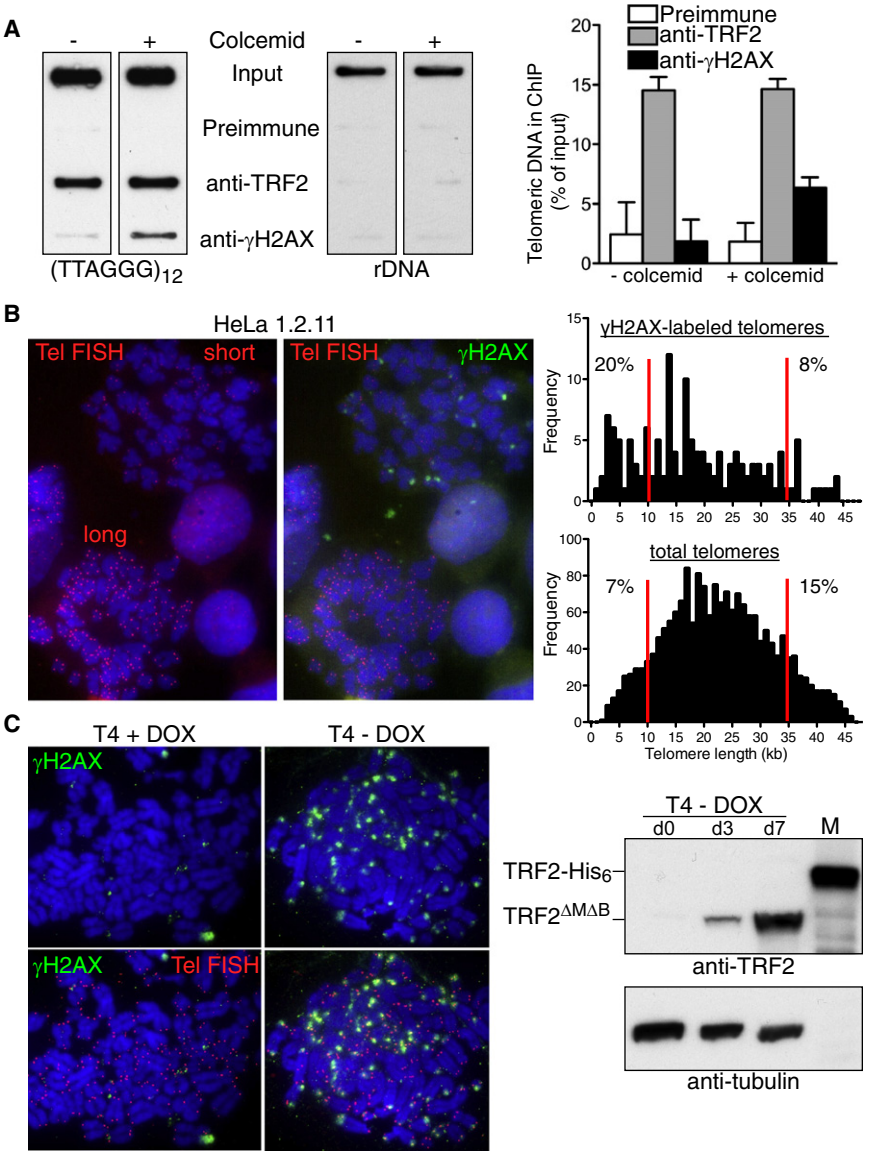

Figure 2. γH2AX Associates Preferentially with Short, Uncapped Telomeres

(A) HeLa 1.2.11 cells were arrested in mitosis with colcemid or remained untreated. ChIP analyses were carried out as described in the Experimental Procedures. Error bars represent SD of three independent experiments.

(B) HeLa 1.2.11 cells were arrested in mitosis with colcemid, and mitotic chromosomes were spread onto glass slides via the cytospin method. Preparations were stained with anti-γH2AX antibodies (green) and a Cy3-conjugated $(CCCTAA)_6$-PNA probe (red). DNA was counterstained with DAPI (blue). For Q-FISH analysis of telomere length distribution, n = 4814 telomeres were analyzed, of which 315 stained positive for γH2AX.

(C) Control cells (T4 + Dox) or cells expressing the human $TRF2^{\Delta M\Delta B}$ variant (T4 – Dox) were arrested in mitosis with colcemid, and mitotic chromosomes were spread onto glass slides. Preparations were stained with anti-γH2AX antibodies (green) and a Cy3-conjugated $(CCCTAA)_6$-PNA probe (red). $TRF2^{\Delta M\Delta B}$ expression was confirmed by western blotting. Recombinant full-length human TRF2-His_6, migrating more slowly because of its epitope tag, served as a specificity control. Tubulin was used as a loading control.

increase in chromosome and chromatid fusions in $p53^{-/-}$ MEFs. Importantly, we observed a significant 4.4-fold increase in the frequency of chromosome and chromatid fusions that displayed telomeric DNA at the fusion site (Figure 3C). End-to-end fusions containing telomeric sequences are a characteristic signature of telomeric dysfunction [10]. These fusions may break in subsequent mitoses, thus starting a bridge-fusion-breakage cycle [17] that may contribute to the overall genomic instability of p53-deficient cells. Our results demonstrate that p53 is required to protect telomeres from end-to-end fusions.

To address whether p53 affects the telomere capping reaction, we synchronized cells from a pair of isogenic human colorectal cancer cell lines, proficient or deleted for *p53* (HCT116 $p53^{+/+}$ or $p53^{-/-}$) [13], by double thymidine block and release. We monitored the occurrence of TIFs at the G2/M transition, 7–11 hr after the second release. At 7 hr, both $p53^{+/+}$ and $p53^{-/-}$ cells had completed DNA replication and stained positive for the G2 specific marker CENP-F [18] (Figure S3). Most cells in both populations exhibited more than two TIFs at this time. By the time cells entered mitosis, as seen by the increase in phosphohistone H3 staining, TIFs were no longer observed in $p53^{+/+}$ cells. In contrast, TIFs remained detectable in most $p53^{-/-}$ cells throughout mitosis and as cells re-entered G1, at 10 hr after release. This suggests that p53 is required for efficient completion of telomere capping and that the p53 response pathway may have an impact on the capping reaction. Alternatively, homologous recombination reactions that are part of telomere capping may become disfavored as $p53^{-/-}$ cells enter mitosis prematurely [19, 20]. As reported previously [13] and as shown here by staining with phosphohistone H3 (Figure S3), a marker for the G2/M transition, mitotic entry of $p53^{-/-}$ cells was somewhat advanced compared to $p53^{+/+}$ cells.

Uncapped Telomeres Trigger ATM- and p53/p21-Dependent G2/M Arrest

To directly address the ability of p53 to delay the G2/M transition in the presence of uncapped telomeres, we disrupted telomere protective structures by depleting components of the telomeric complex in mouse and human cells and compared mitotic indexes between $p53^{+/+}$ and $p53^{-/-}$ cells. $p53^{+/+}$ and $p53^{-/-}$ primary MEFs carrying homozygous floxed *TRF1* alleles ($TRF1^{F/F}$) [21] were infected with retroviruses encoding Cre recombinase or vector control. Deletion of *TRF1*, as monitored by western blotting, resulted in marked telomere uncapping visualized by γH2AX-labeled telomeres (Figure 4A). TIF quantification in interphase cells revealed no impact of p53 status on TIF frequency (data not shown). To analyze mitotic entry of these cells after telomere uncapping, we determined the fraction of cells in mitosis at the indicated times after

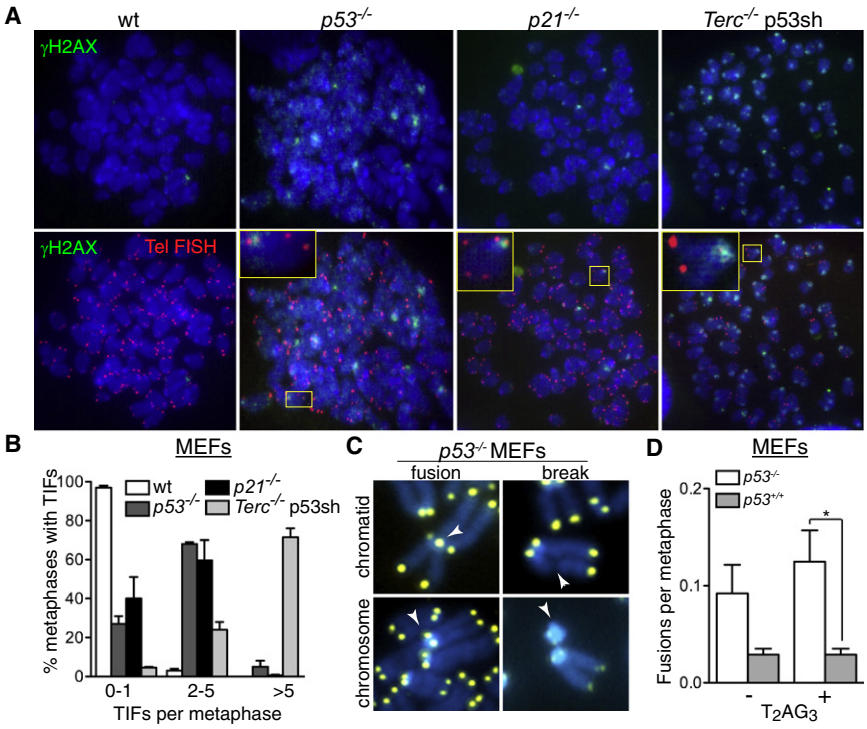

Figure 3. p53 and p21 Prevent Progression into Mitosis in the Presence of Uncapped Telomeres in MEFs

(A) MEFs established from wild-type, $p53^{-/-}$, $p21^{-/-}$, or $Terc^{-/-}$ p53sh embryos were arrested in mitosis with colcemid, and mitotic chromosomes were spread via the cytospin method. Preparations were fixed and stained with anti-γH2AX monoclonal antibody (green). Telomeres were visualized with a Cy3-conjugated $(CCCTAA)_6$-PNA probe (red). DNA was counterstained with DAPI (blue). Insets show enlarged images of the areas marked with yellow rectangles.

(B) TIF frequency was determined by counting the number of foci in 100–150 metaphases. Error bars represent SD of three independent experiments.

(C) Metaphase chromosomes from $p53^{+/+}$ and $p53^{-/-}$ MEFs were stained with DAPI and telomeres were visualized by FISH. Examples of end-to-end fusions with telomeric sequences at the fusion site and DNA breaks are shown.

(D) End-to-end fusions with or without telomeric repeats at the fusion site were quantified in at least 142 metaphases from each genotype. Error bars represent SD of values obtained for three different embryos of each genotype. The p value was calculated with an unpaired two-tailed t test. *$p < 0.05$.

This figure is related to Figure S3.

infection (Figure 4B). $p53^{+/+}$ cells displayed a very low mitotic index after uncapping, compared to *TRF1*-positive control cells. $p53^{-/-}$ cells showed a higher mitotic index in the *TRF1*-proficient background compared to $p53^{+/+}$ cells, and this was not affected after loss of telomere protection by *TRF1* deletion. FACS analysis of DNA content (Figure 4B) confirmed that the low mitotic index in $p53^{-/-}$ cells with uncapped telomeres was due to an arrest of cells in G2/M rather than G1/S.

Similarly, p53 was required to prevent mitotic entry of human cells with uncapped telomeres (Figure S4A). When TRF2 was depleted with siRNA in $p53^{+/+}$ or $p53^{-/-}$ HCT116 cells, the ability of cells to enter mitosis was significantly impaired only in the presence of functional p53. Additionally, human cells depleted of p21 and TRF2 entered mitosis at a higher rate compared to p21-proficient cells (Figure S4B). This suggests that a p53-dependent pathway recognizes uncapped telomeres and delays mitotic entry via activation of p21. Consistent with this idea, we observed p21 induction after siRNA-mediated depletion of TRF2 (Figure S4B).

TIF formation at uncapped telomeres during S phase is ATM dependent [2]. Similarly, we found that mitotic TIFs were strongly reduced when we treated HeLa 1.2.11 cells with the ATM inhibitor Ku55933 (Figure S4C). In comparison, MO59J cells deficient in DNA-PK activity [22] showed similar levels of mitotic TIFs to those of HeLa and MO59K control cells. Instead, Ku55933 addition prevented mitotic TIF formation in MO59J and MO59K cells to the same degree as in HeLa cells. This demonstrates that γH2AX labeling of mitotic telomeres depends on ATM, but not DNA-PK, characteristic for the response to uncapped telomeres.

To gain mechanistic insight into the control of p53 activation at the G2/M transition, we monitored in synchronized human cells ATM-dependent p53 phosphorylation at Ser15, an event known to occur in response to DNA damage [23, 24]. Ser15 phosphorylation occurred in S phase and also at the G2/M transition monitored by FACS analyses of DNA content and phospho-H3 staining (Figure 4C). Concomitant activation of p21 was observed only in G2/M, emphasizing its importance at this stage of the cell cycle. Another target of p53, 14-3-3σ [25], showed a similar induction pattern to that of p21, raising the possibility that 14-3-3σ is also involved in the response to telomere damage. To test this hypothesis, we synchronized U2OS cells that have been depleted of TRF2 by using siRNA (Figure 4D). Although increased ATM-dependent Ser15 p53 phosphorylation, as well as p21 induction, occurred specifically in response to TRF2 depletion, 14-3-3σ expression was not significantly augmented. This suggests that p21, and to a lesser degree 14-3-3σ, act downstream of p53 in response to telomere dysfunction at the G2/M transition.

Traditionally, much research on p53 has focused on its role in regulating cell-cycle arrest at the G1/S transition in response to DNA damage and other types of cellular stress. An ATM- and p53-dependent checkpoint that detects altered telomeric state at the G1/S transition was proposed to act as a regulator of the cellular response to telomere dysfunction [26]. However, several reports also support a role for the p53 pathway at the G2/M transition (reviewed in [25, 27]). Here we provide evidence that telomere uncapping during normal cell-cycle progression triggers a p53-dependent checkpoint at the G2/M transition. The nature of the signal could be the linear telomere structure transiently generated during DNA replication in S phase, which resembles an unrepaired DSB. It has been proposed that telomeres in a linear form trigger a DNA damage response to initiate the reactions required for elongation, processing, and capping [4], and reactions related to those of DNA repair by homologous recombination are required to form a protective t loop structure [20]. Our results suggest that ATM, as a sensor of linear telomeres, at least in part uses p53 as an effector to delay mitotic entry and halt the cell cycle in a state conducive for the capping processes to be completed. The physiologic p53 response to uncapped

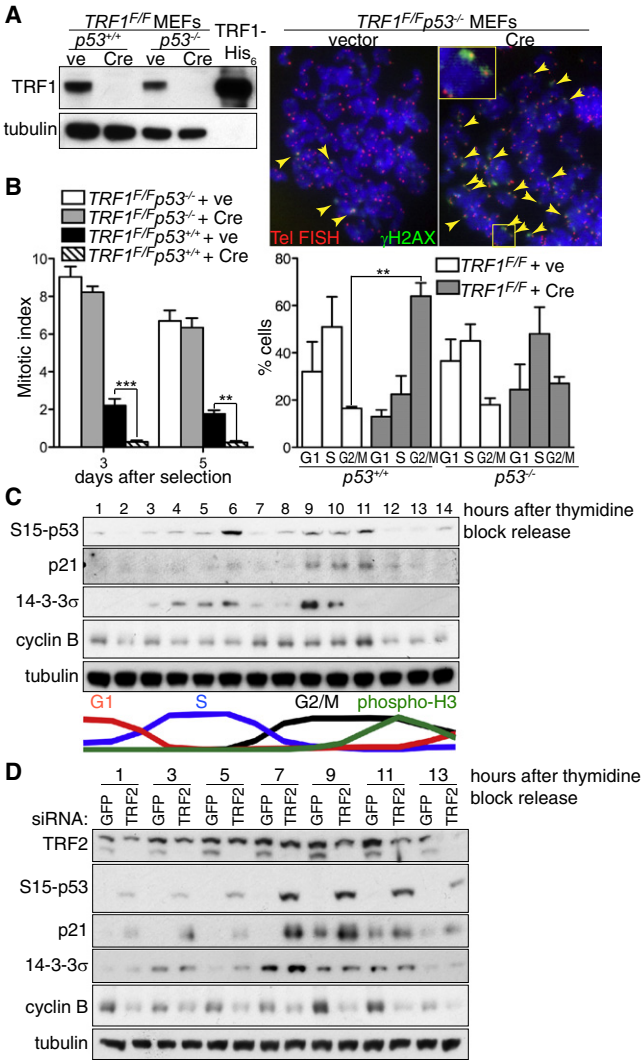

Figure 4. p53 Controls the G2/M Transition in Response to Uncapped Telomeres and Undergoes ATM-Dependent Phosphorylation

(A) Western blot detection of mouse TRF1 in primary *p53*$^{+/+}$*TRF1*$^{F/F}$ and *p53*$^{-/-}$*TRF1*$^{F/F}$ MEFs of the indicated genotypes treated with empty pBabe vector (ve) or Cre recombinase (Cre) 3 days after selection. Recombinant human TRF1-His$_6$ served as a specificity control. Tubulin was used as loading control. *p53*$^{-/-}$*TRF1*$^{F/F}$ MEFs were arrested in mitosis with colcemid and then mitotic chromosomes were spread via the cytospin method and stained with anti-γH2AX monoclonal antibody (green). Telomeres were visualized with a Cy3-conjugated (CCCTAA)$_6$-PNA probe (red). DNA was counterstained with DAPI (blue). Yellow arrows indicate TIFs.

(B) The mitotic index was determined in n = 350–500 cells for each genotype, treatment, and time point. FACS analysis of DNA content was performed on propidium iodide-stained cells. Error bars represent SD of two independent experiments. p values were calculated with an unpaired two-tailed t test. **p < 0.01 and ***p < 0.001.

(C) U2OS cells were synchronized at the G1/S transition via a double thymidine block. Extracts prepared from cells at the indicated times after release were immunoblotted as indicated.

(D) U2OS cells transfected with control GFP or TRF2 siRNAs were grown for 24 hr before synchronization by double thymidine block and release. Extracts prepared at the indicated times after release were immunoblotted as shown.

This figure is related to Figure S4.

telomeres, which naturally occur in every round of cell division after DNA replication, extends our understanding of this important tumor suppressor.

Experimental Procedures

Cell Culture and Treatments

Human T4 [10], HeLa 1.2.11, HeLa OHIO, U2OS, HCT116 wild-type and *p53*$^{-/-}$ cells [13], and MO59J and MO59K [22] (all obtained from Cancer Research UK Cell Services) were cultivated in monolayers in Dulbecco's modified Eagle's medium (DMEM) (Invitrogen) supplemented with antibiotics (penicillin and streptomycin, Sigma Aldrich) and 10% fetal bovine serum (FBS, Invitrogen). Primary MEFs were isolated from day 13.5 embryos embryos as previously described [28] and cultivated in DMEM medium (Invitrogen) supplemented with antibiotics (penicillin and streptomycin, Sigma Aldrich) and 10% FBS (Invitrogen). *p21*$^{-/-}$ MEFs [14] were a gift from M. Serrano (CNIO). Isogenic wild-type and *p53*$^{-/-}$ MEFs, isogenic *TRF1*$^{F/F}$ *p53*$^{-/-}$ and *TRF1*$^{F/F}$ *p53*$^{+/+}$, and MEFs established from C57BL6 embryos of 4th generation (G4) *Terc*$^{-/-}$ immortalized by p53 depletion (shp53 [29]) have been previously described [12, 16, 21]. ATM inhibitor Ku-55933 ([30]; a gift from G. Smith) was added at 10 μM final concentration for 1 hr prior to collection. Mitotic cell arrest was carried out by addition of 0.1 μg/ml colcemid (GIBCO) to human cells and 0.2–0.3 μg/ml to MEF cultures, followed by 4–12 hr incubation at 37°C. The synchronization of HeLa 1.2.11, HCT116, and U2OS cells was performed with a double thymidine block. In brief, exponentially growing cells were arrested by addition of thymidine (2 mM) to the growth media for 16 hr, followed by two washes in HBSS and release into fresh media for 10 hr. Cells were then arrested a second time by addition of thymidine (2 mM) and 16 hr incubation, then washed as above and released into fresh media.

Antibodies

The following antibodies were used for immunoblotting: rabbit polyclonal antisera raised against human TRF2 [31], mouse TRF2 (2390 [32]), human histone H3 (a gift from A. Verreault), Ser15-p53 (Cell Signaling), and human p21 (C-19, Santa Cruz); and mouse monoclonal antibodies raised against phosphorylated ATM-Ser1981 (Cell Signaling), mouse TRF1 (TRF-78, Abcam), p53 (DO-1, Santa Cruz Biotechnology), 14-3-3σ (Upstate), and α-tubulin [31] (Cancer Research UK Monoclonal Antibody Service). Additional antibodies used for imunoflourescence detection were mouse monoclonal antibodies raised against MDC1 (Abcam) and phosphorylated histone H2AX-Ser 139 (Upstate) and a rabbit polyclonal antiserum raised against 53BP1 (Novus) and CENP-F (Abcam). Antibodies used in ChIP analyses were rabbit polyclonal antibodies anti-phosphorylated histone H2AX-Ser 139 (Upstate) and anti-human TRF2.

Preparation of Metaphase Spreads

Mitotic cells were collected by mitotic shake off and swollen in hypotonic buffer (10 mM Tris-HCl, pH 7.5, 10 mM NaCl, 5 mM $MgCl_2$) at 37°C for 5 min. For IF-FISH, cells were either spun onto coverslips via a cytospin centrifuge (Cytospin 4, Fisher) or spread across a slide presoaked in 2% paraformaldehyde as described [33] and dried. For Q-FISH, cells were fixed in a freshly prepared 3:1 mix of methanol:glacial acetic acid. Nuclear preparations were dropped onto slides presoaked in 45% acetic acid and left to dry overnight.

Immunofluorescence and FISH

Metaphase spreads prepared as above were fixed in 4% paraformaldehyde with 0.1%–0.5% Triton X-100 in PBS, permeabilized with 0.5% Triton X-100 in PBS, and subjected to immunofluorescence staining as described [31]. In brief, metaphase spreads were incubated in antibody dilution buffer (1% goat serum, 0.3% BSA, 0.005% Triton X-100 in PBS) for 10 min, then in primary antibody overnight. After three washes in antibody dilution buffer supplemented with 0.005% Triton X-100, secondary antibody was added for 1 hr. All antibody incubations were at room temperature. Samples were then washed and fixed again in 4% paraformaldehyde in PBS. After three washes in PBS, slides were briefly dried at room temperature. FISH was performed as described [31] with 15 μg/ml Cy3-conjugated [CCCTAA]$_6$-PNA telomeric probe (Applied Biosystems). Chromosomes were visualized with DAPI.

Q-FISH, Mitotic Index, and Chromosome Analyses

Primary MEFs were isolated from day 13.5 embryos from *p53*$^{-/-}$ [12] and *p21*$^{-/-}$ mice [14] as described [34], passaged once and treated with 0.1 μg/ml colcemid for 4 hr, trypsinized, and fixed as above for metaphase spreads. Q-FISH analyses and statistical analyses of chromosomal aberrations and telomere length were carried out as described [28, 31]. Fifty anaphases per cell line from two independent cell samples of each

genotype were scored. One fusion event was defined as the result of the joining of two or more chromosomes. The end-to-end fusion index was calculated as the number of events per total number of metaphases. For determining the mitotic index, dried metaphase spreads were mounted in DAPI and visualized by fluorescence microscopy. Nuclei with condensed, evenly stained chromosomes were counted as mitotic. Between 350 and 500 nuclei were scored for each time point.

Supplemental Information

Supplemental Information includes four figures and Supplemental Experimental Procedures and can be found with this article online at doi:10.1016/j.cub.2010.01.046.

Acknowledgments

We thank I. Hickson for sharing unpublished results, M. Terradas for help with MO59K and J cell lines, M. Woodcock for FACS analyses, and M. Eid for initial metaphase spread preparations. M. Serrano, B. Vogelstein, and T. De Lange kindly supplied reagents. M.A.B.'s laboratory is funded by the Spanish Ministry of Innovation and Science. Work in M.T.'s laboratory is supported by Cancer Research UK, Breast Cancer Campaign, and The Royal Society.

Received: November 11, 2009
Revised: January 12, 2010
Accepted: January 14, 2010
Published online: March 11, 2010

References

1. Palm, W., and de Lange, T. (2008). How shelterin protects mammalian telomeres. Annu. Rev. Genet. *42*, 301–334.
2. Takai, H., Smogorzewska, A., and de Lange, T. (2003). DNA damage foci at dysfunctional telomeres. Curr. Biol. *13*, 1549–1556.
3. d'Adda di Fagagna, F., Reaper, P.M., Clay-Farrace, L., Fiegler, H., Carr, P., Von Zglinicki, T., Saretzki, G., Carter, N.P., and Jackson, S.P. (2003). A DNA damage checkpoint response in telomere-initiated senescence. Nature *426*, 194–198.
4. Verdun, R.E., Crabbe, L., Haggblom, C., and Karlseder, J. (2005). Functional human telomeres are recognized as DNA damage in G2 of the cell cycle. Mol. Cell *20*, 551–561.
5. d'Adda di Fagagna, F., Teo, S.H., and Jackson, S.P. (2004). Functional links between telomeres and proteins of the DNA-damage response. Genes Dev. *18*, 1781–1799.
6. Stucki, M., and Jackson, S.P. (2006). gammaH2AX and MDC1: Anchoring the DNA-damage-response machinery to broken chromosomes. DNA Repair (Amst.) *5*, 534–543.
7. Mochan, T.A., Venere, M., DiTullio, R.A., Jr., and Halazonetis, T.D. (2004). 53BP1, an activator of ATM in response to DNA damage. DNA Repair (Amst.) *3*, 945–952.
8. Canela, A., Vera, E., Klatt, P., and Blasco, M.A. (2007). High-throughput telomere length quantification by FISH and its application to human population studies. Proc. Natl. Acad. Sci. USA *104*, 5300–5305.
9. Meier, A., Fiegler, H., Muñoz, P., Ellis, P., Rigler, D., Langford, C., Blasco, M.A., Carter, N., and Jackson, S.P. (2007). Spreading of mammalian DNA-damage response factors studied by ChIP-chip at damaged telomeres. EMBO J. *26*, 2707–2718.
10. van Steensel, B., Smogorzewska, A., and de Lange, T. (1998). TRF2 protects human telomeres from end-to-end fusions. Cell *92*, 401–413.
11. Stott, F.J., Bates, S., James, M.C., McConnell, B.B., Starborg, M., Brookes, S., Palmero, I., Ryan, K., Hara, E., Vousden, K.H., and Peters, G. (1998). The alternative product from the human CDKN2A locus, p14(ARF), participates in a regulatory feedback loop with p53 and MDM2. EMBO J. *17*, 5001–5014.
12. Jacks, T., Remington, L., Williams, B.O., Schmitt, E.M., Halachmi, S., Bronson, R.T., and Weinberg, R.A. (1994). Tumor spectrum analysis in p53-mutant mice. Curr. Biol. *4*, 1–7.
13. Bunz, F., Dutriaux, A., Lengauer, C., Waldman, T., Zhou, S., Brown, J.P., Sedivy, J.M., Kinzler, K.W., and Vogelstein, B. (1998). Requirement for p53 and p21 to sustain G2 arrest after DNA damage. Science *282*, 1497–1501.
14. Brugarolas, J., Chandrasekaran, C., Gordon, J.I., Beach, D., Jacks, T., and Hannon, G.J. (1995). Radiation-induced cell cycle arrest compromised by p21 deficiency. Nature *377*, 552–557.
15. Hao, L.Y., Strong, M.A., and Greider, C.W. (2004). Phosphorylation of H2AX at short telomeres in T cells and fibroblasts. J. Biol. Chem. *279*, 45148–45154.
16. Herrera, E., Samper, E., Martín-Caballero, J., Flores, J.M., Lee, H.-W., and Blasco, M.A. (1999). Disease states associated with telomerase deficiency appear earlier in mice with short telomeres. EMBO J. *18*, 2950–2960.
17. Maser, R.S., and DePinho, R.A. (2002). Connecting chromosomes, crisis, and cancer. Science *297*, 565–569.
18. Badie, S., Liao, C., Thanasoula, M., Barber, P., Hill, M.A., and Tarsounas, M. (2009). RAD51C facilitates checkpoint signaling by promoting CHK2 phosphorylation. J. Cell Biol. *185*, 587–600.
19. Esashi, F., Christ, N., Gannon, J., Liu, Y., Hunt, T., Jasin, M., and West, S.C. (2005). CDK-dependent phosphorylation of BRCA2 as a regulatory mechanism for recombinational repair. Nature *434*, 598–604.
20. Verdun, R.E., and Karlseder, J. (2006). The DNA damage machinery and homologous recombination pathway act consecutively to protect human telomeres. Cell *127*, 709–720.
21. Martínez, P., Thanasoula, M., Muñoz, P., Liao, C., Tejera, A., McNees, C., Flores, J.M., Fernández-Capetillo, O., Tarsounas, M., and Blasco, M.A. (2009). Increased telomere fragility and fusions resulting from TRF1 deficiency lead to degenerative pathologies and increased cancer in mice. Genes Dev. *23*, 2060–2075.
22. Allalunis-Turner, J., Barron, G.M., and Day, R.S., 3rd. (1997). Intact G2-phase checkpoint in cells of a human cell line lacking DNA-dependent protein kinase activity. Radiat. Res. *147*, 284–287.
23. Siliciano, J.D., Canman, C.E., Taya, Y., Sakaguchi, K., Appella, E., and Kastan, M.B. (1997). DNA damage induces phosphorylation of the amino terminus of p53. Genes Dev. *11*, 3471–3481.
24. Girard, P.M., Riballo, E., Begg, A.C., Waugh, A., and Jeggo, P.A. (2002). Nbs1 promotes ATM dependent phosphorylation events including those required for G1/S arrest. Oncogene *21*, 4191–4199.
25. Taylor, W.R., and Stark, G.R. (2001). Regulation of the G2/M transition by p53. Oncogene *20*, 1803–1815.
26. Karlseder, J., Broccoli, D., Dai, Y., Hardy, S., and de Lange, T. (1999). p53- and ATM-dependent apoptosis induced by telomeres lacking TRF2. Science *283*, 1321–1325.
27. Kastan, M.B., and Bartek, J. (2004). Cell-cycle checkpoints and cancer. Nature *432*, 316–323.
28. Blasco, M.A., Lee, H.W., Hande, M.P., Samper, E., Lansdorp, P.M., DePinho, R.A., and Greider, C.W. (1997). Telomere shortening and tumor formation by mouse cells lacking telomerase RNA. Cell *91*, 25–34.
29. Dirac, A.M., and Bernards, R. (2003). Reversal of senescence in mouse fibroblasts through lentiviral suppression of p53. J. Biol. Chem. *278*, 11731–11734.
30. Hickson, I., Zhao, Y., Richardson, C.J., Green, S.J., Martin, N.M.B., Orr, A.I., Reaper, P.M., Jackson, S.P., Curtin, N.J., and Smith, G.C.M. (2004). Identification and characterization of a novel and specific inhibitor of the ataxia-telangiectasia mutated kinase ATM. Cancer Res. *64*, 9152–9159.
31. Tarsounas, M., Muñoz, P., Claas, A., Smiraldo, P.G., Pittman, D.L., Blasco, M.A., and West, S.C. (2004). Telomere maintenance requires the RAD51D recombination/repair protein. Cell *117*, 337–347.
32. Muñoz, P., Blanco, R., Flores, J.M., and Blasco, M.A. (2005). XPF nuclease-dependent telomere loss and increased DNA damage in mice overexpressing TRF2 result in premature aging and cancer. Nat. Genet. *37*, 1063–1071.
33. McGuinness, B.E., Hirota, T., Kudo, N., Peters, J.-M., and Nasmyth, K. (2005). Shugoshin prevents dissociation of cohesin from centromeres during mitosis in vertebrate cells. PLoS Biol. *3*, 433–449.
34. Palmero, I., and Serrano, M. (2001). Induction of senescence by oncogenic Ras. Methods Enzymol. *333*, 247–256.